

A Simple Relativistic Correction to the Nuclear Spin–Spin Coupling Constant

Jana Khandogin and Tom Ziegler*

Department of Chemistry, The University of Calgary, 2500 University Drive NW,
Calgary, AB T2N 1N4, Canada

Received: July 23, 1999; In Final Form: October 19, 1999

We present two relativistic correction schemes to account for the relativistic effects on one-bond metal–ligand couplings. On the basis of the Pauli Hamiltonian, the first method is a direct analogue to the nonrelativistic spin–spin coupling approach. In the second method, however, only the s-orbital contraction of the coupling metal atom is taken into account in computing the Fermi-contact contribution. These schemes are applied to the calculation of metal–ligand reduced coupling constants ${}^1K(M-L)$ in some group 4 and 12 hydrides, alkyl complexes, and cyano complexes, as well as some platinum ammine and platinum phosphine complexes. It is shown that the second approximate method, a refined version of the “hydrogen-like” relativistic correction suggested by Pyykkö, gives greater improvement over the nonrelativistic values and agrees better with experiments. Finally, the connection between the trans influence and coupling constants is discussed in the context of some square-planar platinum complexes.

I. Introduction

The rapid development of high-speed computing resources and the recent advances in ab initio and density functional theory (DFT) have enabled the theoretical prediction and interpretations of NMR chemical shifts and indirect spin–spin coupling constants. Since NMR parameters are used extensively by experimental chemists to identify and probe the structure of inorganic and organic compounds, the importance of their theoretical study cannot be overestimated. Over the past few years, a large number of papers have been published on calculations of NMR chemical shifts or shieldings. The interested reader may refer to the recent review articles by Helgaker¹ and Jameson.² In contrast, the theoretical aspects of nuclear spin–spin couplings have not yet attracted as much attention. So far, approaches based on the traditional ab initio methods such as CCSD,^{3,4} MCSCF,⁵ and MP2⁶ have been developed. Because of the high computational demand of these methods, the applications are, however, restricted to selected diatomic molecules, second-row hydrides and a few small organic molecules.¹ More recently, the implementations in the DFT framework were reported by Malkin et al.⁷ as well as by Dickson and Ziegler.⁸ The latter implementation was later applied by us⁹ to the study of nuclear spin–spin couplings in a series of transition-metal complexes. This work has demonstrated the ability of the currently used nonrelativistic DFT-based techniques to provide quantitative predictions of the coupling constants between 3d transition metals and directly bonded ligand atoms such as carbon, oxygen, fluorine, and phosphorus. The fact that the nuclear spin–spin interactions involving oxygen and fluorine are less well described by the present methodology can be attributed to the deficiency of the existing exchange–correlation functionals in dealing with large electron correlations¹⁰ and to the lack of the current dependency.¹¹ Further, the comparison of the nonrelativistic predictions with experimental coupling values for 5d-transition-metal systems in this work⁹ suggested that relativistic treatment is required for a quantitative description.

The study of relativistic effects on the indirect nuclear spin–spin coupling has rarely been attempted in the literature. In the

seventies, Pyykkö et al. introduced a multiplicative “hydrogen-like” relativistic correction factor, originating from Breit, to account for the relativistic effects in Fermi-contact contribution to the nuclear couplings.^{12–14} Later, Pyykkö developed a relativistic analogue¹⁵ of Ramsey’s spin–spin coupling expression,¹⁶ which in the early eighties was incorporated into the semiempirical relativistic extended Hückel (REX) method.¹⁷ With this approach, Pyykkö and Wiesenfeld calculated one-bond couplings in some small main-group compounds.^{17,18} The relativistic increase in ${}^1J(M-H)$ and ${}^1J(X-C)$ was found to be approximately 30% for SnH_4 and $\text{Sn}(\text{CH}_3)_4$, as well as more than 125% for the analogous lead compounds. They also found that the relativistic isotropic coupling constant is dominated invariably by the term, which has the nonrelativistic Fermi-contact (FC) origin. Recently, Kirpekar et al.¹⁹ has applied the MCSCF method to investigate spin–orbit effects on the coupling constants in XH_4 . The spin–orbit contribution to ${}^1J(M-H)$ was shown to be very small, amounting to about 1% for SnH_4 . The findings by Pyykkö and Kirpekar et al. imply that the relativistic alteration of the coupling constant may be recovered by a scalar relativistic correction to the FC term without resorting to the two- or four-component relativistic coupling formalism. In the present work, we shall follow this idea and develop some simple relativistic correction schemes to account for the relativistic effects on the metal–ligand coupling constant.

In Ramsey’s nonrelativistic nuclear spin–spin coupling theory,¹⁶ there are four terms contributing to the indirect nuclear spin–spin coupling constant: the Fermi-contact and spin dipolar (SD) terms arising from the spin of the electron and the para- and diamagnetic spin–orbit terms originating from the orbital motion of the electron. The FC operator takes effect whenever there is a finite electron density (s orbitals) at one nucleus and creates a net spin density (in a closed-shell molecule), which then interacts with the magnetic dipole of the second nucleus. The FC term gives in most cases the dominant contribution and is particularly sensitive to relativistic effects as a result of the orbital and bond length contractions. Bond length shortening can be taken into account by making use of experimental

geometries in the calculation. In the present paper, the remaining relativistic effects on the FC term can be accounted for to a first approximation by the following two approaches based on the nonrelativistic coupling formalism. The first approach involves the quasi-relativistic Pauli Hamiltonian^{20–23} and is a straightforward analogue to the nonrelativistic method. The second scheme treats the effect of (s) orbital contraction on the FC term explicitly by replacing s-orbitals in the self-consistent nonrelativistic Kohn–Sham orbitals by the relativistic ones without changing the orbital expansion coefficients. We will describe in detail these two relativistic correction schemes in section II. In section III, we will test these schemes by calculating the metal–ligand coupling constants ${}^1J(\text{M–L})$ in a series of group 12 and group 14 alkyl, cyano, and hydrido complexes. In section IV, we will further validate the relativistic correction schemes on couplings involving a platinum atom and examine the connection between trans influence and spin–spin couplings.

II. Computational Methods and Details

A. Quasi-Relativistic Kohn–Sham Method. Perhaps one of the most successful approaches to include relativity due to the first-order ($1/c^2$) relativistic operators is the frozen-core-based quasi-relativistic (QR) method. In the QR method, unlike in other perturbation approaches, the relativistic corrections to the valence density due to the first-order relativistic operators are calculated variationally up to all orders. Consequently, the total Kohn–Sham electronic energy can be written as a functional of the quasi-relativistically modified density:²⁴

$$E^{\text{QR}}[\rho^{\text{QR}}] = E^{\text{NR}}[\rho^{\text{QR}}] + \sum_i^{n_{\text{val}}} \int d\vec{r}_1 \Psi_i^{\text{QR}*} h^{\text{QR}} \Psi_i^{\text{QR}} \quad (1)$$

where the sum in the second term runs over occupied valence electrons and the constant core terms are omitted from both of the terms here. Given in atomic units, the first-order relativistic operator

$$h^{\text{QR}} = h^{\text{MV}} + h^{\text{Dar}} + h^{\text{SO}} \quad (2)$$

contains the mass–velocity operator

$$h^{\text{MV}} = -\frac{1}{8c^2} \vec{p}^4 \quad (3)$$

the Darwin operator

$$h^{\text{Dar}} = \frac{1}{8c^2} \Delta(V_{\text{N}} + V_{\text{el}}) \quad (4)$$

and the spin–orbit (SO) operator

$$h^{\text{SO}} = \frac{1}{4c^2} \vec{\sigma} \cdot [\nabla(V_{\text{N}} + V_{\text{el}}) \times \vec{p}] \quad (5)$$

where V_{N} and V_{el} refer to the nuclear and electron potential, respectively. $\vec{\sigma}$ is the electron spin operator. h^{QR} is the one-electron form of the Pauli Hamiltonian. However, combined with the frozen-core approximation, the QR method elegantly bypasses the unboundness problem inherent in the Pauli Hamiltonian. In eq 1, $E^{\text{NR}}[\rho^{\text{QR}}]$ is the nonrelativistic energy expressed in terms of the quasi-relativistic Kohn–Sham orbitals

that are obtained as the solution to the quasi-relativistic Kohn–Sham equation

$$f^{\text{QR}} \Psi_i^{\text{QR}}(\vec{r}_1) = \epsilon_i^{\text{QR}} \Psi_i^{\text{QR}}(\vec{r}_1) \quad (6)$$

by requiring that $E^{\text{QR}}[\rho^{\text{QR}}]$ is minimized with respect to the quasi-relativistic valence density $\rho_{\text{V}}^{\text{QR}}$ given as

$$\rho_{\text{V}}^{\text{QR}}(\vec{r}_1) = \sum_i^{n_{\text{val}}} \Psi_i^{\text{QR}*}(\vec{r}_1) \Psi_i^{\text{QR}}(\vec{r}_1) \quad (7)$$

The QR Kohn–Sham operator can be written as

$$f^{\text{QR}}(\vec{r}_1) = h^{\text{NR}}(\vec{r}_1) + h^{\text{QR}}(\vec{r}_1) \quad (8)$$

with $h^{\text{NR}}(\vec{r}_1)$ representing the nonrelativistic Kohn–Sham operator.²⁵ For closed-shell systems, spin–orbit effects can often be neglected and $h^{\text{QR}}(\vec{r}_1)$ is replaced by the scalar relativistic (SR) operator $h^{\text{SR}}(\vec{r}_1)$ that includes only the MV and Darwin terms. The related SR Kohn–Sham operator serves as a basis of our relativistic modification schemes.

B. Formulation of the Scalar Relativistic Correction Schemes. In nonrelativistic theory, the four operators (FC, PSO, DSO, and SD) that give rise to the nuclear spin–spin coupling can be derived from the nonrelativistic Hamiltonian by applying the minimal coupling ($\vec{p} \rightarrow \vec{p} + e\vec{A}$) to the momentum operator and including an extra term that accounts for the interaction between the electron spin and the magnetic field due to nuclei ($\vec{\sigma} \cdot \vec{B}$). These operators are widely known as hyperfine terms, since they describe the interaction between electrons and nuclei. These interactions then give rise to the indirect nuclear spin–spin coupling via the so-called double perturbation. Rigorously, the relativistic spin–spin coupling constant should be calculated from the relativistic hyperfine terms, which can be derived from the Dirac Hamiltonian or some approximate two-component Hamiltonian such as ZORA.²⁶ Because relativistic hyperfine terms require at least a two-component wave function, calculation of the spin–spin coupling is often very time-consuming. The goal of this work is, however, to devise some approximate schemes that can account for most of the relativistic effects on the nuclear coupling while still maintaining the computational ease of the nonrelativistic approach. As stated in the previous section, the mass–velocity correction and Darwin term introduce the major scalar relativistic modifications to the electronic structure. This would in turn influence the nuclear spin–spin couplings even if the hyperfine interactions stay formally unaltered. On the basis of these considerations, our first approach (we shall call it SRI) to estimate relativistic effects on the coupling constant involves the scalar QR Hamiltonian and utilizes the nonrelativistic hyperfine operators. Here, the scalar relativistic reduced spin–spin coupling tensor is expressed as the second derivative of the scalar QR energy:

$$K(\text{A,B})_{ij}^{\text{SRI}} = \left. \frac{\partial^2 E^{\text{SR}}}{\partial \mu_{\text{A}}^i \partial \mu_{\text{B}}^j} \right|_{\mu_{\text{A}} = \mu_{\text{B}} = 0} \quad \text{with} \quad i, j \in \{x, y, z\} \quad (9)$$

In eq 9, E^{SR} is the total scalar relativistic electronic energy, i and j run over the three Cartesian components, and μ_{A}^i and μ_{B}^j represent the magnetic moments due to nuclei A and B, respectively. The evaluation of $K(\text{A,B})_{ij}^{\text{SRI}}$ follows the same procedures⁹ as for the nonrelativistic coupling tensor, except that now the unperturbed orbitals are derived from the QR Hamiltonian. Also, the FC perturbation is now added to the QR

KS operator to yield the perturbed spin density matrix. Thus, the isotropic DSO and PSO contributions can be written in SI units as

$$K(A,B)_{ii}^{\text{SRI,DSO}} = \frac{\mu_0^2 e^2}{16\pi^2 m_e} \sum_k^{\text{occ}} \int \Psi_k^{\text{QR}*}(\vec{r}_1) \frac{(\vec{r}_A \cdot \vec{r}_B) - r_A^i r_B^i}{r_A^3 r_B^3} \Psi_k^{\text{QR}}(\vec{r}_1) d\vec{r}_1 \quad (10)$$

and

$$K(A,B)_{ii}^{\text{SRI,PSO}} = -2 \left(\frac{\mu_0 \beta}{2\pi} \right)^2 \sum_k^{\text{occ}} \sum_l^{\text{vir}} \frac{\int \Psi_k^{\text{QR}*}(\vec{r}_1) h^{(\mu_A^{\text{A,PSO}})} \Psi_l^{\text{QR}}(\vec{r}_1) d\vec{r}_1}{\epsilon_k^{\text{QR}} - \epsilon_l^{\text{QR}}} \times \int \Psi_l^{\text{QR}*}(\vec{r}_1) h^{(\mu_B^{\text{B,PSO}})} \Psi_k^{\text{QR}}(\vec{r}_1) d\vec{r}_1 \quad (11)$$

where

$$h^{(\mu_A^{\text{A,PSO}})} = \frac{1}{r_A^3} (\vec{r}_A \times \vec{\nabla}) \quad \text{and} \quad h^{(\mu_B^{\text{B,PSO}})} = \frac{1}{r_B^3} (\vec{r}_B \times \vec{\nabla}) \quad (12)$$

In the equations above, Ψ_k^{QR} denotes the unperturbed QR KS orbitals obtained via eq 6 and β and μ_0 represent the Bohr magneton and vacuum permeability, respectively. The final formula for the FC contribution is given by

$$K(A,B)_{ii}^{\text{SRI,FC}} = \frac{2\mu_0 \beta^{\text{AO'sAO's}}}{3} \sum_r \sum_s P_{rs}^{\text{QR},(\mu_A^{\text{A,FC}})} \phi_r^{\text{QR}}(\vec{r} = \vec{r}_B) \phi_s^{\text{QR}}(\vec{r} = \vec{r}_B) \quad (13)$$

with $P_{rs}^{\text{QR},(\mu_A^{\text{A,FC}})}$ being the first-order spin-density matrix on the basis of QR atomic orbitals $\phi_r^{\text{QR}}(\vec{r})$ and is determined via

$$P_{rs}^{\text{QR},(\mu_A^{\text{A,FC}})} = \frac{P_{rs}^{\text{QR},\alpha}(\lambda) - P_{rs}^{\text{QR},\beta}(\lambda)}{\lambda} \quad (14)$$

where $P_{rs}^{\alpha}(\lambda)$ and $P_{rs}^{\beta}(\lambda)$ are the perturbed density matrix for α and β spins, respectively. These density matrices are constructed from the perturbed KS orbitals obtained by solving the KS equations with a finite Fermi-contact perturbation self-consistently:

$$\{f^{\text{QR}}[\rho^{\text{QR}}] + \lambda \delta(r_A) \sigma_z\} \Psi_k^{\text{FC}} = \epsilon_k^{\text{FC}} \Psi_k^{\text{FC}} \quad (15)$$

Here, λ is the finite perturbation parameter, $f^{\text{QR}}[\rho^{\text{QR}}]$ is the scalar KS operator as a functional of the unperturbed QR density, and $\delta(r_A)$ is the Dirac delta function. The subscript FC is used for KS orbital functions and energies to emphasize that they are perturbed by the Fermi-contact term.

Relativity has impact on each of the three contributions to the nuclear coupling. However, the relativistic correction to the FC contribution is presumably the largest for two reasons. First, the FC term is the predominant contributor to the total coupling. Second, since the FC operator describes the electron–nuclear interaction at the nuclear site, the FC contribution is most sensitive to relativistic effects. According to eq 13, the FC contribution suffers the relativistic orbital contraction, which affects both the first-order spin-density matrix $P_{rs}^{\text{QR},(\mu_A^{\text{A,FC}})}$ and the atomic orbital values: $\phi_r(\vec{r} = \vec{r}_B)$ and $\phi_s(\vec{r} = \vec{r}_B)$. However, since we are dealing with couplings involving only one heavy atom,

we can deliberately choose the light atom as the perturbing center A and neglect the relativistic effects on the first-order density matrix due to the perturbation of the light atom. In other words, we need to take into account only the relativistic effects on $\phi_r(\vec{r} = \vec{r}_B)$ and $\phi_s(\vec{r} = \vec{r}_B)$. Our previous experience has shown that choosing the lighter atom as the perturbing center gave rise to results that are numerically stable with respect to computational parameters.⁹ On the basis of these considerations, we can write down an approximate form for the relativistically corrected FC contribution as

$$K(A,B)_{ii}^{\text{SRII,FC}} = \frac{2\mu_0 \beta^{\text{AO'sAO's}}}{3} \sum_r \sum_s P_{rs}^{\text{NR},(\mu_A^{\text{A,FC}})} \phi_r^{\text{QR}}(\vec{r} = \vec{r}_B) \phi_s^{\text{QR}}(\vec{r} = \vec{r}_B) \quad (16)$$

where $\phi_r^{\text{QR}}(\vec{r} = \vec{r}_B)$ is obtained from the QR calculation for atomic B, and $P_{rs}^{\text{NR},(\mu_A^{\text{A,FC}})}$ corresponds to the nonrelativistic form of eq 14. In contrast to the SRI approach, the SRII scheme is computationally less expensive, because only QR atomic calculation is required in addition to computing the nonrelativistic spin–spin coupling.

C. Computational Details. All calculations were performed using the NMR spin–spin coupling code,^{8,27} which was implemented within the Amsterdam density functional (ADF) package.^{28,29} The SRII correction was carried out with an auxiliary program. We chose the all-electron triple- ζ plus double polarization (ADF set V) basis for the coupling ligand atoms, while for the metal and other ligand atoms the frozen-core triple- ζ plus single polarization (ADF set IV) basis sets were employed. The valence space for the coupling transition and main-group metals contains subvalence in addition to the true valence electrons. In the self-consistent finite perturbation procedure of calculating FC contribution, the ligand atoms were always used as the perturbing center⁹ and the perturbation parameter was set to 10^{-3} .

In the calculation of coupling constants involving main-group elements, the experimental structure parameters from the following references are used: ref 30 for CH₄; ref 31 for SiH₄, GeH₄, and SnH₄; ref 32 for Zn(CH₃)₂ and Cd(CH₃)₂; ref 33 for Hg(CH₃)₂; ref 34 for [Zn(CN)₄]²⁻; ref 35 for [Cd(CN)₄]²⁻; ref 36 for [Hg(CN)₄]²⁻. For PbH₄ the theoretically optimized bond length from ref 37 is adopted.

In the calculation of couplings involving the platinum atom, the structural data for [Pt(NH₃)₄]²⁺ and Pt(PF₃)₄ are taken from refs 38 and 39, respectively. The metal–ligand bond distances as well as angles between them for *cis*-, *trans*-PtCl₂(PMe₃)₂, and *cis*-, *trans*-PtCl₄(PEt₃)₂ are taken from ref 40, while the metric data for the ligands are taken from compilations of crystal structure data.⁴¹ For *cis*- and *trans*-PtCl₂(NH₃)₂, we assume $R(\text{Pt–N}) = 2.05 \text{ \AA}$, $R(\text{Pt–Cl}) = \text{\AA}$, $\theta(\text{NPtN}) = 90^\circ$, $R(\text{N–H}) = 1.01 \text{ \AA}$, and $\theta(\text{NPtN}) = 109.5^\circ$ based on the crystal structure data^{41,42} and theoretical calculation.⁴³ The structural data for *cis*- and *trans*-PtH₂(PMe₃)₂ are taken from ref 44, where the Pt–H bond distance for the *cis* isomer is computationally optimized.

III. Results and Discussions

A. Couplings to Main-Group Metals. To test the scalar relativistic correction schemes described in the last section, we calculated the one-bond coupling constants for a series of group 4 and 12 compounds. Table 1 presents the total coupling constants obtained with the nonrelativistic method (K^{NR}) and the quasi-relativistic scalar corrections SRI (K^{SRI}) and SRII

TABLE 1: Calculated One-Bond Reduced Coupling Constants (in $10^{19} \text{ J}^{-1} \text{ T}^2$) for Some Main-Group 2 and 16 Compounds Using the Nonrelativistic Method and SRI and SRII Schemes

molecule	coupling	K^{exp}	K^{NR}	K^{SRI}	K^{SRII}
SiH ₄	$K(\text{Si}-\text{H})$	84.79 ^{na}	88 ^e	87 ^f	89 ^g
GeH ₄	$K(\text{Ge}-\text{H})$	232 ^b	188	207	217
SnH ₄	$K(\text{Sn}-\text{H})$	431 ^a	294	304	293
PbH ₄	$K(\text{Pb}-\text{H})$	923 ^c	501	629	851
Ge(CH ₃) ₄	$K(\text{Ge}-\text{C})$		86	89	108
Sn(CH ₃) ₄	$K(\text{Sn}-\text{C})$	302 ^d	195	187	201
Pb(CH ₃) ₄	$K(\text{Pb}-\text{C})$	396 ^d	72	-147	207
Zn(CH ₃) ₂	$K(\text{Zn}-\text{C})$		299	309	349
Cd(CH ₃) ₂	$K(\text{Cd}-\text{C})$	797 ^e	485	488	634
Hg(CH ₃) ₂	$K(\text{Hg}-\text{C})$	126 ^e	666	460	1309
[Zn(CN) ₄] ²⁻	$K(\text{Zn}, \text{C})$	465 ^e	405	449	458
[Cd(CN) ₄] ²⁻	$K(\text{Cd}, \text{C})$	855 ^e	648	794	821
[Hg(CN) ₄] ²⁻	$K(\text{Hg}, \text{C})$	2832 ^e	1039	1471	1857

^a From ref 59. ^b Form ref 60. ^c Taken from the measured coupling constant $^1J(\text{Pb}-\text{H})$ in $\text{PbH}(\text{CH}_3)_3$.⁶¹ ^d From ref 62. ^e From ref 63. ^f $K^{\text{NR}} = K_{\text{FC}}^{\text{NR}} + K_{\text{DSO}}^{\text{NR}} + K_{\text{FC}}^{\text{NR}}$, where $K_{\text{FC}}^{\text{NR}}$, $K_{\text{DSO}}^{\text{NR}}$, and $K_{\text{FC}}^{\text{NR}}$ are evaluated according to eqs 10, 11, and 13, respectively, over nonrelativistic orbitals. ^g $K^{\text{SRI}} = K_{\text{FC}}^{\text{SRI}} + K_{\text{DSO}}^{\text{SRI}} + K_{\text{FC}}^{\text{SRI}}$, where $K_{\text{FC}}^{\text{SRI}}$, $K_{\text{DSO}}^{\text{SRI}}$, and $K_{\text{FC}}^{\text{SRI}}$ are evaluated according to eqs 10, 11, and 13, respectively, over scalar relativistic orbitals. ^f $K^{\text{SRII}} = K_{\text{FC}}^{\text{NR}} + K_{\text{DSO}}^{\text{NR}} + K_{\text{FC}}^{\text{SRII}}$, where $K_{\text{FC}}^{\text{SRII}}$ is evaluated according to eq 16.

(K^{SRII}) in comparison with experimental values (K^{exp}). Overall, the SRII scheme gives better results than the SRI method. It can also be seen that relativity already starts to take effect on couplings involving the fourth-row elements such as Zn and Ge. An increase of 15% seems to be an average for couplings to H or C. For the sixth-row elements Pb and Hg, the SRII scheme enhances the total coupling constants by 70%, 96%, and 70% for PbH_4 , $\text{Hg}(\text{CH}_3)_4$, and $[\text{Hg}(\text{CN})_4]^{2-}$, respectively. With the experimental values as reference, a factor of 2 seems to be appropriate as a rough estimate of the relativistic increase. If this were true, then we could ascribe the large discrepancy between the predicted and measured coupling constant in $\text{Pb}(\text{CH}_3)_4$ to the underestimation before relativistic effects are taken into account. According to the nonrelativistic calculation, a relativistic increase factor of 550% would be anticipated to recover the experimental value, which seems to be unreasonable.

Because of their simplicity, group 4 tetrahydrides are perhaps the best model compounds for investigation of relativistic effects due to a heavy metal on the spin-spin coupling. For the purpose of assessing the quality of the DFT-based calculations and studying the effects of electron correlation, we carried out calculations with several different XC functionals. These include LDA⁴⁵ and GGA-type functionals due to Becke and Perdew (BP86),^{46,47} Perdew and Wang (PW91),⁴⁸ and Becke, Lee, Yang, and Parr (BLYP).^{46,49} It is found that LDA gives results roughly 10% smaller than BP86, while other GGA functionals yield values very close to BP86. Therefore, we shall focus on comparison of the BP86 and LDA results. In Table 2, all contributions obtained with BP86 and LDA without relativistic corrections are presented. We also show the few available numbers from the MCSCF calculations.¹⁹ Comparing LDA with BP86, we note that all FC and PSO contributions from the BP86 calculations are larger in magnitude. The DSO contributions are numerically very small and will therefore not be discussed. The change in the FC contribution induced by the gradient correction (also called nonlocal correction) to the density functional can be attributed to the change in electron density due to the gradient correction. Fan and Ziegler⁵⁰ have shown that nonlocal corrections generally increase the density at the core region and the valence tail. Since the FC contribution is

TABLE 2: Comparison of DFT, HF, and Post-HF Calculations^a for One-Bond Coupling Constants in Group 4 Tetrahydrides

complex	method	$K_{\text{FC}}^{\text{NR}}$	$K_{\text{FC}}^{\text{NR}}$	$K_{\text{DSO}}^{\text{NR}}$	$K_{\text{tot}}^{\text{NR}}$	$K_{\text{corr}}^{\text{rel } b}$	K^{exp}
SiH ₄	BP86	88.3	-0.170	0.013	88.1	0.5	84.79
	LDA	75.9	-0.144	0.014	75.7	1.2	
	RPA	96.64	-0.138	0.0084	96.51	0.025	
GeH ₄	CAS B	78.21	-0.084	0.0126	78.14		
	BP86	189.0	-0.482	0.019	188.5	28.2	232
	LDA	170.0	-0.362	0.016	169.65	25.6	
	RPA	300.74	-0.547	0.0238	300.22	0.169	
SnH ₄	CAS B	232.66	-0.499	0.0238	232.18		
	BP86	295.5	-1.221	0.013	294.3	-1.3	431
	LDA	266.7	-1.074	0.013	265.6	0.6	
	RPA	485.48	-1.394	0.0067	484.09	4.71	
PbH ₄	RAS B	421.75	-1.227	0.0067	420.53		
	BP86	504.3	-2.81	0.010	501.5	349.2	923
	LDA	442.1	-2.54	0.010	439.6	312.3	

^a Results taken from ref 19; RPA refers to the lower level random-phase approximation (RPA) while CAS B and RAS B refer to the correlated results with CAS B and RAS B as reference MCSCF wave functions. ^b Scalar relativistic corrections with the SRII scheme are listed for BP86 and LDA calculations. The spin-orbit corrections are shown for RPA results.

extremely sensitive to the change in the core region of the valence orbitals, the increase due to nonlocal corrections is readily understandable. The fact that the BP86 results compare better with experimental values is another proof that nonlocal corrections are important for describing sensitive molecular properties such as nuclear couplings. Comparing DFT results with Hartree-Fock (HF) and post-HF results, we find that for the PSO and DSO contributions, which are singlet properties, DFT agrees extremely well with the HF-based methods. For FC contributions, a triplet property, DFT generally gives lower values than RPA- and MCSCF-based approaches. The only exception is SiH_4 , where BP86 yields a higher coupling constant than CAS B does. It is interesting to note that the nonrelativistic MCSCF calculations agree perfectly with experiments for GeH_4 and SnH_4 and as a consequence leave no room for any relativistic corrections in contrast to DFT calculations. However, as mentioned before, it seems peculiar that our scalar relativistic scheme does not give any correction to the coupling $^1K(\text{Sn}-\text{H})$. Also, even with relativistic correction, DFT-based $^1K(\text{Ge}-\text{H})$ is smaller than the measured value. All these facts indicate that there is an underestimation on the nonrelativistic level for the DFT approach. However, since, as seen from Table 2, the spin-orbit effects are of no importance for all couplings, and there are no scalar relativistic ab initio results available, it remains unclear to which extent the DFT results are underestimated.

Finally, we shall give some comments on the relativistic effects on the spin-spin coupling and try to understand why the SRII correction scheme works better. As already known,⁵¹ effects of relativity manifest themselves in both the molecular geometry and electronic structure. The former can be observed in the contraction of the bond length when one (or both) of the bonding atoms belongs to the fifth-row or higher elements in the periodic table. The latter gives rise to the orbital contraction and stabilization (s and p) as well as the orbital expansion and destabilization (d and f). It seems surprising that although the relativistic effects on KS orbitals are fully taken into account in our SRI scheme, it gives less improvement than the SRII scheme where only the s-contraction is accounted for. This may be attributed to the deficiency in the current implementation of the quasi-relativistic approach, where the valence orbitals are subjected to the relativistic core potential but orthogonalized

TABLE 3: Calculated One-Bond Reduced Coupling Constants (in $10^{19} \text{ J}^{-1} \text{ T}^2$) for Some Platinum Complexes Using the Nonrelativistic Method and Scalar Relativistic Correction SRI and SRII Schemes

molecule	coupling	K^{exp}	K^{NR}	K^{SRI}	K^{SRII}
$[\text{Pt}(\text{NH}_3)_4]^{2+}$	$K(\text{Pt}-\text{N})$	1089 ^a	605	599	999
<i>c</i> -PtCl ₂ (NH ₃) ₂	$K(\text{Pt}-\text{N})$	1154 ^b	411	150	730
<i>t</i> -PtCl ₂ (NH ₃) ₂	$K(\text{Pt}-\text{N})$	1059 ^b	496	368	891
Pt(PF ₃) ₄	$K(\text{Pt}-\text{P})$	6215 ^c	2981	3770	5433
<i>c</i> -PtCl ₂ (PMe ₃) ₂	$K(\text{Pt}-\text{P})$	3316 ^d	1487	1609	2286
<i>t</i> -PtCl ₂ (PMe ₃) ₂	$K(\text{Pt}-\text{P})$	2267 ^d	867	892	1433
<i>c</i> -PtH ₂ (PMe ₃) ₂	$K(\text{Pt}-\text{P})$	1786 ^d	893	654	1474
<i>t</i> -PtH ₂ (PMe ₃) ₂	$K(\text{Pt}-\text{P})$	2472 ^d	1200	839	1832
<i>c</i> -PtCl ₄ (PEt ₃) ₂	$K(\text{Pt}-\text{P})$	1976 ^e	946	978	1602
<i>t</i> -PtCl ₄ (PEt ₃) ₂	$K(\text{Pt}-\text{P})$	1386 ^e	695	626	1131

^a From ref 64. ^b From ref 65. ^c From ref 66. ^d From ref 55. ^e From ref 54.

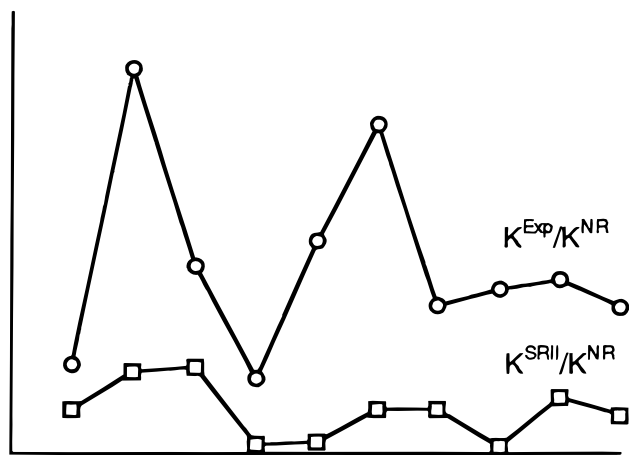


Figure 1. Correlation between the calculated and experimentally predicted relativistic increase in coupling constants for some platinum complexes.

onto the nonrelativistic core orbitals. Also, it is difficult to justify whether the simple incorporation of the nonrelativistic hyperfine terms to the Pauli Hamiltonian is an appropriate approach to satisfactorily treat the relativistic effects on the spin–spin coupling. On the other hand, the consequences of the approximate SRII approach are more apparent, since it only accounts for the s-orbital contraction, which is the predominant relativistic effect on the contact-type nuclear spin–spin interactions.

B. Couplings to Platinum. To examine the validity of the proposed relativistic correction scheme SRII for couplings involving transition metals, we have performed calculations on some platinum complexes. Table 3 presents both predicted and experimental ${}^1K(\text{Pt}-\text{N})$ and ${}^1K(\text{Pt}-\text{P})$ for some platinum amine and platinum phosphine complexes. Again, it can be seen that the SRII correction is able to recover most of the anticipated relativistic increase with an average deviation of around 25% from experiment, whereas the SRI method fails completely.

By comparing $K^{\text{SRII}}/K^{\text{NR}}$ with $K^{\text{exp}}/K^{\text{NR}}$, Figure 1 shows how the calculated relativistic correction is related to the experimentally predicted relativistic increase. From the shape of the curve $K^{\text{exp}}/K^{\text{NR}}$ it is obvious that the extent of relativistic modification depends on the chemical environment of the coupling nucleus. This can certainly not be described by the “hydrogen-like” relativistic correction of Pyykkö,^{12–14} where a multiplicative factor is assigned for each heavy metal and applied on top of the nonrelativistically calculated total coupling constants. In contrast, our SRII correction can mimic the trend of relativistic influence in different ligand environments to a

certain degree. Evidently, our correction is more flexible than the “hydrogen-like” correction.

The thermodynamic trans influence, defined as the extent to which a ligand labilizes the bond opposite to itself in the ground state, is a well-established concept in transition-metal chemistry.^{52,53} The trans influence is experimentally measurable through the use of X-ray crystallography, vibrational spectroscopy, nuclear magnetic resonance, nuclear quadrupole resonance, and photoelectron spectroscopy. The order of trans influence obtained by these techniques for common ligands is similar but not unique since it reflects one or more aspects of the electronic structure of the complex. Maybe the most widely known trans influence series is provided by the determination of the bond length $\text{M}-\text{A}$ that is trans to the influencing ligand L . Consequently, ligands such as amine, chloride, phosphine, and hydride in square-planar Pt(II) complexes can be placed in the order of their structural trans influence as⁵² $\text{NH}_3 \approx \text{Cl}^- < \text{PR}_3 < \text{H}^-$. In our discussion, we will refer to the influencing ligand L as the ligand that exerts a stronger trans influence according to this series.

The connection between the trans influence and the magnitude of NMR coupling constants for stereoisomers of platinum square-planar and octahedral systems was discussed in refs 52, 54, and 55. Thus, for the complexes $\text{PtCl}_2(\text{PR}_3)_2$, a greater value of ${}^1K(\text{Pt}-\text{P})$ is always observed for the cis isomers than for the trans isomers. It was proposed that the trans influence of a ligand is to reduce the s-character of the platinum hybrid orbital and consequently to decrease the coupling between platinum and phosphorus.^{56,57} However, until now, no first-principles calculation has addressed this issue. Therefore, it seems worthwhile to investigate this relation through DFT-based calculations. The first important question in this conjunction is whether the difference in the coupling constant for cis and trans isomers can be ascribed to the difference in the bond distance due to the structural trans influence as addressed in ref 54. For this purpose, we shall examine how the calculated ${}^1K(\text{Pt}-\text{P})$ changes at various bond lengths, angles, and geometrical arrangements.

It can be seen that, if $R(\text{Pt}-\text{P})$ is increased from 2.25 Å in the equilibrium geometry of *cis*-Cl₂(PMe₃)₂ (**1**), to 2.31 Å in **2**, ${}^1K(\text{Pt}-\text{P})$ decreases from 1609 to 1471 ($10^{19} \text{ J}^{-1} \text{ T}^2$). At this new bond distance $R(\text{Pt}-\text{P})$, if $R(\text{Pt}-\text{Cl})$ is shortened to 2.31 Å, and the angles $\theta(\text{P}-\text{Pt}-\text{P})$ and $\theta(\text{Cl}-\text{Pt}-\text{Cl})$ are arranged to be 90° in **3**, ${}^1K(\text{Pt}-\text{P})$ reduces further to 1203 ($10^{19} \text{ J}^{-1} \text{ T}^2$), which is about 25% lower than the value at the equilibrium geometry **1**. Finally, keeping the bond lengths and angles fixed, if the position of one chlorine ligand is exchanged with that of one phosphine ligand (**4**, the equilibrium geometry of *trans*-PtCl₂(PMe₃)₂), ${}^1K(\text{Pt}-\text{P})$ reduces further by about 20% to 892 ($10^{19} \text{ J}^{-1} \text{ T}^2$). Similar calculations have also been conducted for PtH₂(PMe₃)₂ isomers. They reveal a variation of ${}^1K(\text{Pt}-\text{P})$ from 654 at the cis geometry, **5**, over 430, at the bond distance and angles from the trans configuration, **6**, to 839 ($10^{19} \text{ J}^{-1} \text{ T}^2$), at the trans geometry, **7**. Thus, apart from the outcome of the structural trans influence, there is a more important electronic factor that determines the spin–spin coupling in these square-planar systems. This factor explains the change in the coupling in going from the cis isomer **3** to the trans isomer **4**, or from **6** to **7**. We shall in the following borrow the idea from Burdett and Albricht⁵⁸ to rationalize this electronic influence.

For an ideal trans complex with symmetry D_{2h} , the σ interactions between metal and ligands give rise to three ligand-based occupied MO's: $1a_g$, $2a_g$, and b_{3u} , and the corresponding metal-based antibonding virtual orbitals (see Figure 3). Here, it is assumed that the trans influencing ligand is L_2 , identical to

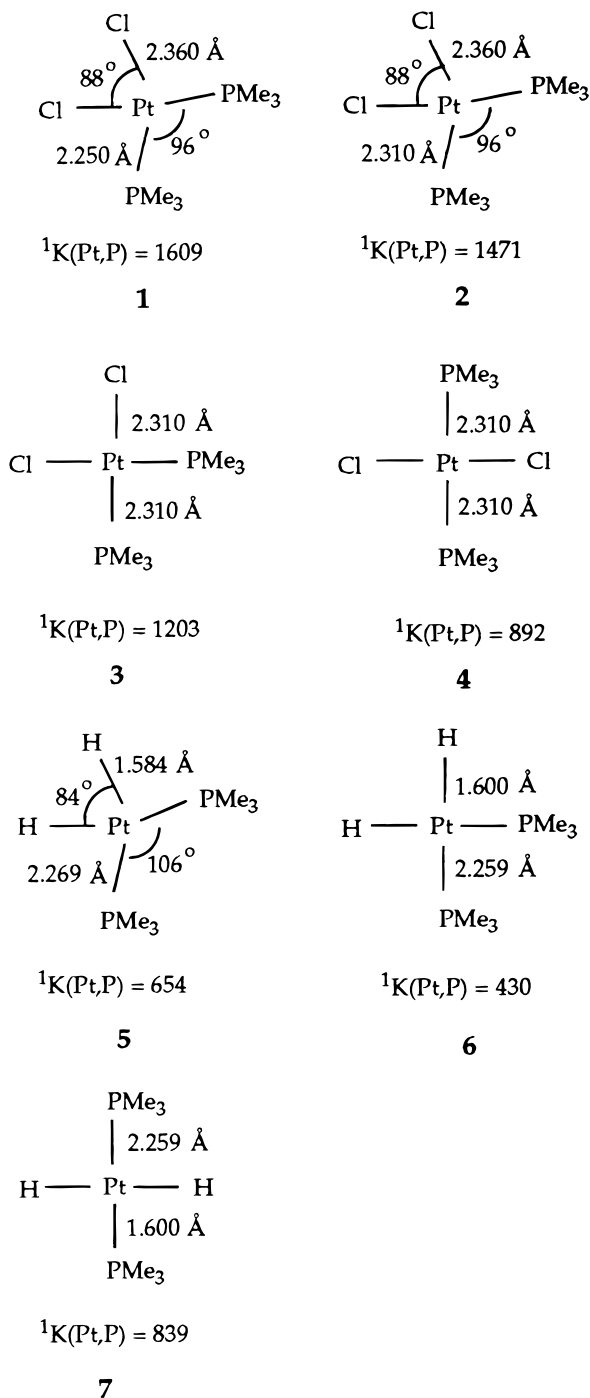


Figure 2. Dependence of the coupling constants (calculated with SRI correction scheme) on the structure parameters.

L_4 , and the influenced ligand is L_1 , identical to L_3 . Obviously, $2a_g$ is the orbital that contributes to the spin–spin coupling.⁹ Now if the ligand L_2 is replaced with L_2' , which has a higher electronegativity or a lower σ -donor ability, the symmetry of the system is reduced to C_{2v} , with $L_2'-M-L_4$ as the C_2 axis. Consequently, the initial b_{3u} orbital becomes a total symmetrical orbital $3a_1$ and can be perturbed by the virtual orbital $2a_1^*$ to form a new orbital, which represents the bonding interaction of the metal hybrid sp_x orbital with the σ ligand orbitals trans to each other (L_2' and L_4), as shown in Figure 4.

This perturbation is favored because of the small energy gap between the high-lying occupied orbital $3a_1$ and the low-lying virtual orbital $2a_1^*$. Since L_2 has a higher electronegativity, the phase of the mixing is determined such that the resultant orbital

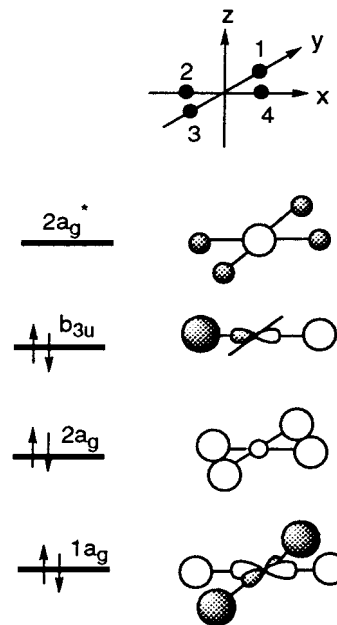


Figure 3. Important σ interactions in a trans planar complex with symmetry D_{2h} .

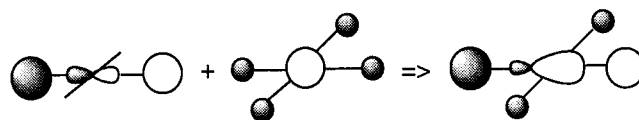


Figure 4. Polarization of the virtual orbital on the trans σ bond $L'-M-L''$ in a $trans\text{-ML}_2L'L''$ complex with symmetry C_{2v} .

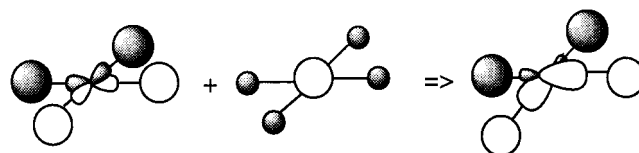


Figure 5. Polarization of the virtual orbital on the trans σ bond $L-M-L'$ in a $cis\text{-ML}_2L'_2$ complex with symmetry C_{2v} .

has a larger electron density at L_2 . It is clear from the shape of this orbital that there is a large overlap population between the metal s -orbital and the σ -orbital at L_4 , and hence it can add to the FC term of the $M-L_4$ spin–spin coupling. In other words, $^1K(M-L_4)$ becomes larger if the trans ligand L_2 is replaced by a weaker σ -donor ligand L_2' . This predicts that $^1K(M-L_4)$ in $trans\text{-PtCl}_2(\text{PMe}_3)\text{Cl}$ should be larger relative to that in $trans\text{-PtCl}_2(\text{PMe}_3)_2$, as Cl^- is a weaker σ -donor.

Let us examine now the situation when the position of L_2 is switched with that of L_1 . In this case, the molecule still transforms as C_{2v} , but with the C_2 axis cutting through the two identical ligands. Consequently, the initial $2a_g^*$ orbital will mix with an occupied orbital that is a linear combination of the initial orbitals b_{2u} and b_{3u} and gives rise to a new bonding orbital that contains a large overlap population between the metal s -orbital and both of the σ -orbitals from L_4 and L_2 (see Figure 5). Therefore, the coupling $^1K(M-L_4)$ is anticipated to increase with respect to the original trans configuration. This explains why $^1K(M-P)$ is larger than in $cis\text{-PtCl}_2(\text{PMe}_3)_2$ in its trans isomer.

After establishing the link between electronic trans influence, σ -donor ability, and the magnitude of spin–spin coupling constants, we can understand the results for other stereoisomers of Pt(II) and Pt(IV) complexes. Our calculations show a slightly larger coupling for $trans$ - than for $cis\text{-PtCl}_2(\text{NH}_3)_2$ (see Table 3). However, experimental values give a reversed trend. This

can be explained, as the σ -donor abilities of Cl^- and NH_3 are very close and our approximate method may not be able to pick up the fine difference. For hydridophosphine complexes, both theoretically and experimentally the trans isomer exhibits larger $^1K(\text{Pt}-\text{P})$ since the hydrido ligand is a stronger σ -donor than phosphine. Moving to the octahedral Pt(IV) complexes $\text{PtCl}_4(\text{PEt}_3)_2$, it is noted that $\text{Pt}-\text{P}$ coupling is much smaller than the analogous square-planar complexes. The correlation of the oxidation state with the magnitude of the coupling constant is, however, accidental. As pointed out in ref 9 complexes with a larger coordination number generally should have smaller coupling constants, owing to the smaller normalization factor $1/\sqrt{n}$, where n represents the coordination number.

IV. Concluding Remarks

On the basis of the nonrelativistic hyperfine operators, two approximate frozen-core scalar relativistic corrections are devised to account for the major relativistic effects on one-bond metal–ligand nuclear spin–spin coupling constants. In the first scheme, SRI, the quasirelativistic approach is incorporated into the nonrelativistic coupling calculation. In the second scheme, SRII, a refined version of Pyykkö's "hydrogen-like" hyperfine correction is used, which only involves the correction of the s-orbital value at the heavy nucleus in the evaluation of the Fermi-contact contribution.

The calculations have revealed that SRII gives significant improvement over SRI for couplings to sixth-row main-group elements. It is also able to satisfactorily recover the bulk of the relativistic increase for couplings to platinum and reproduce the experimental trends in different ligand environment due to the relativistic effects, whereas the SRI scheme fails almost completely. We rationalize this as the SRII method accounts for the s-orbital contraction, which is the predominant relativistic effect on the contact-type nuclear spin–spin interactions. However, one of the limitations of this scheme is that it can treat couplings involving only one heavy nucleus. Also, owing to its highly qualitative nature, an approach to the systematic improvement of the correction is not obvious. Therefore, a rigorous approach departing from a relativistic hyperfine operator would be desirable.

Finally, as an interesting application, the connection between the structural trans influence and the magnitude of coupling constants has been explored on the basis of the calculations. It has been found that, although the metal–ligand bond distance and angles influence the magnitude of the coupling, the major factor that gives rise to the difference between cis and trans configuration is of electronic nature. This can be attributed to the change in the overlap population between the metal s- and ligand σ -orbitals under the influence of a trans ligand, which is caused by the polarization of the antibonding virtual orbital (between metal s- and ligand σ -orbitals) on the occupied trans σ bonds.

Acknowledgment. This work has been supported by the National Science and Engineering Research Council of Canada (NSERC), as well as by the donors of the Petroleum Research Fund, administered by the American Chemical Society (ACS-PRF No. 31205-AC3). The NOVA Graduate Scholarship (to J.K.) is greatly acknowledged.

References and Notes

- Helgaker, T.; Jaszunski, M.; Ruud, K. *Chem. Rev.* **1999**, *99*, 293.
- Jameson, C. J.; Dios, A. C. In *A Specialist Periodical Report, Nuclear Magnetic Resonance*; Webb, G. A., Ed.; Royal Society of Chemistry: London, 1999; Vol. 28, Chapter 2.
- Oddershede, J.; Geertsen, J.; Scuseria, G. E. *J. Phys. Chem.* **1988**, *92*, 3056.
- Perera, S. A.; Sekino, H.; Bartlett, R. J. *J. Chem. Phys.* **1994**, *101*, 2186.
- Vahtras, O.; Agren, H.; Jorgensen, P.; Jensen, H. J. A.; Padkjaer, S. B.; Helgaker, T. *J. Chem. Phys.* **1992**, *96*, 6120.
- Fukui, H.; Miura, K.; Matsuda, H.; Baba, T. *J. Chem. Phys.* **1992**, *97*, 2299.
- Malkin, V. G.; Malkina, O. L.; Salahub, D. R. *Chem. Phys. Lett.* **1994**, *221*, 91.
- Dickson, R. M.; Ziegler, T. *J. Phys. Chem.* **1996**, *100*, 5286.
- Khandogin, J.; Ziegler, T. *Spectrochim. Acta* **1999**, *55*, 607.
- Malkina, O. L.; Salahub, D. R.; Malkin, V. G. *J. Chem. Phys.* **1996**, *105*, 8793.
- Malkin, V. G.; Malkina, O. L.; Erikson, L. A.; Salahub, D. R. In *Modern Density Functional Theory: A Tool for Chemistry*; Politzer, P., Seminario, J. M., Eds.; Elsevier: Amsterdam, 1995; pp 273–347.
- Pyykkö, P.; Pajanne, E. *Phys. Lett.* **1971**, *35A*, 53.
- Pyykkö, P.; Pajanne, E.; Inokuti, M. *Int. J. Quantum Chem.* **1973**, *7*, 785.
- Pyykkö, P.; Jokisaari, J. *Chem. Phys.* **1975**, *10*, 293.
- Pyykkö, P. *Chem. Phys.* **1977**, *22*, 289.
- Ramsey, N. F. *Phys. Rev.* **1953**, *91*, 303.
- Pyykkö, P.; Wiesenfeld, L. *Mol. Phys.* **1981**, *43*, 557.
- Pyykkö, P. *J. Organomet. Chem.* **1982**, *232*, 21.
- Kirpekar, S.; Jensen, H. J. A.; Oddershede, J. *Theor. Chim. Acta* **1997**, *95*, 35.
- Snijders, J. G.; Baerends, E. J. *Mol. Phys.* **1978**, *36*, 1789.
- Snijders, J. G.; Baerends, E. J.; Ros, P. *Mol. Phys.* **1979**, *1909*.
- Boerrigter, P. M. Quasirelativistic Method. Ph.D. Thesis, Vrije University Amsterdam, 1987.
- Ziegler, T.; Tschinke, V.; Baerends, E. J.; Snijders, J. G.; Ravenek, W. *J. Phys. Chem.* **1989**, *93*, 3050.
- Ziegler, T.; Snijders, J. G.; Baerends, E. J. *Chem. Phys. Lett.* **1980**, *75*, 1.
- Ziegler, T. *Chem. Rev.* **1991**, *91*, 651.
- Lenche, E. v.; Baerends, E. J.; Snijders, J. G. *J. Chem. Phys.* **1993**, *99*, 4597.
- Khandogin, J. Internal report: NMR spin–spin coupling code for ADF2.3. July 1998.
- Baerends, E. J.; Ellis, D. E.; Ros, P. *Chem. Phys.* **1973**, *2*, 41.
- Te Velde, G.; Baerends, E. J. *J. Comput. Phys.* **1992**, *99*, 84.
- Bennett, B.; Rayness, W. T.; Anderson, C. T. *Spectrochim. Acta* **1989**, *45A*, 821.
- Dyall, K. G.; Taylor, P. R.; Faegri, K. J.; Patridge, H. *J. Chem. Phys.* **1991**, *95*, 2583.
- Suryanarayana, K.; Stoicheff, B. P.; Turner, R. *Can. J. Phys.* **1960**, *38*, 1516.
- Kashiwabara, K.; Konaka, S.; Iijima, T.; Kimura, M. *Bull. Chem. Soc. Jpn.* **1973**, *46*, 407.
- Sequeira, A.; Chidambaram, R. *Acta Crystallogr.* **1965**, *20*, 910.
- Ziegler, B.; Babel, D. Z. *Naturforsch.* **1991**, *42B*, 47.
- Thiele, G.; Grossmann, J.; Pürzer, A. W. Z. *Naturforsch.* **1986**, *41B*, 1346.
- Barandiarán, Z.; Seijo, L. *J. Chem. Phys.* **1994**, *101*, 4049.
- Rochon, F. D.; Melanson, R. *Acta Crystallogr., Sect. C* **1991**, *47*, 2300.
- Marriott, J. C.; Salthouse, J. A.; Ware, M. J.; Freeman, J. M. *Chem. Commun.* **1970**, *1*, 595.
- Hitchcock, P. B.; Jacobson, B.; Pidcock, A. J. *Organomet. Chem.* **1977**, *136*, 397.
- Allen, F. H.; Kennard, O.; Taylor, R. *Acc. Chem. Res.* **1983**, *16*, 6.
- Millburn, G. H.; Truter, M. R. *J. Chem. Soc.* **1966**, 1609.
- Basch, H.; Krauss, M.; Stevens, W. J.; Cohen, D. *Inorg. Chem.* **1985**, *24*, 3313.
- Packett, D. L.; Jensen, C. M.; Cowan, R. L.; Strouse, C. E.; Trogler, W. C. *Inorg. Chem.* **1985**, *24*, 3578–3583.
- Vosko, S. H.; Wilk, L.; Nusair, M. *Can. J. Phys.* **1980**, *58*, 1200.
- Becke, A. *Phys. Rev. A* **1988**, *38*, 3098.
- Perdew, J. P. *Phys. Rev. B* **1986**, *33*, 8822.
- Perdew, J. P. *Phys. Rev. B* **1992**, *46*, 6671.
- Lee, C.; Yang, W.; Parr, R. G. *Phys. Rev. B* **1988**, *37*, 785.
- Fan, L.; Ziegler, T. *J. Chem. Phys.* **1991**, *95*, 7401.
- Pyykkö, P. *Chem. Rev.* **1988**, *88*, 563.
- Appleton, T. G.; Clark, H. C.; Manzer, L. E. *Coord. Chem. Rev.* **1973**, *10*, 335–422.
- Shustorovich, E. M.; Portai-Koshits, M. A.; Buslaev, Y. A. *Coord. Chem. Rev.* **1975**, *17*, 1–98.
- Pregosin, P. S.; Kunz, R. W. In *NMR Basic Principles and Progress*; Diehl, P., Fluck, E., Kosfeld, R., Eds.; Springer-Verlag: Berlin, 1979; Vol. 16.

- (55) Pregosin, P. S. In *Annual Reports on NMR Spectroscopy*; Webb, G. A., Ed.; Academic Press: London, 1986; Vol. 17.
- (56) Pidcock, A.; Richards, R. E.; Venanzi, L. M. *J. Chem. Soc. A* **1966**, 1707.
- (57) Allen, F. H.; Pidcock, A.; Waterhouse, C. R. *J. Chem. Soc. A* **1970**, 2087.
- (58) Burdett, J. K.; Albright, T. A. *Inorg. Chem.* **1979**, *18*, 2112–2120.
- (59) Dreeskamp, H. Z. *Naturforsch.* **1964**, *19*, 139.
- (60) Wilkins, A. L.; Watkinson, P. J.; MacKay, K. M. *J. Chem. Soc., Dalton Trans.* **1987**, 2365.
- (61) Schumann, C.; Dreeskamp, H. *J. Magn. Reson.* **1970**, *3*, 204.
- (62) Wrackmeyer, B.; Horchler, K. In *Annual Reports in NMR Spectroscopy*; Webb, Ed.; Academic Press: London, 1989; Vol. 22, pp 249–306.
- (63) Wu, G.; Kroeker, S.; Wasylishen, R. E. *Inorg. Chem.* **1995**, *34*, 1595.
- (64) Nee, M.; Roberts, J. D. *Biochemistry* **1982**, *21*, 4920.
- (65) Appleton, T. G.; Bailey, A. J.; Barnham, K. J.; Hall, J. R. *Inorg. Chem.* **1992**, *31*, 3077–3082.
- (66) Hao, N.; McGlinchey, M. J.; Sayer, B. G.; Schrobilgen, G. J. *J. Magn. Reson.* **1982**, *46*, 158.